Computational model for the analysis of cartilage and cartilage tissue constructs

Computational model for the analysis of cartilage and cartilage tissue constructs

David W. Smith[1,*], **Bruce S. Gardiner**[1], **John B. Davidson**[1], and **Alan J. Grodzinsky**[2]

[1]School of Computer Science and Software Engineering, University of Western Australia, Crawley, WA, Australia

[2]Center for Biomedical Engineering, Massachusetts Institute of Technology, Cambridge, MA, USA

Abstract

We propose a new non-linear poroelastic model that is suited to the analysis of soft tissues. In this paper the model is tailored to the analysis of cartilage and the engineering design of cartilage constructs. The proposed continuum formulation of the governing equations enables the strain of the individual material components within the extracellular matrix (ECM) to be followed over time, as the individual material components are synthesized, assembled and incorporated within the ECM or lost through passive transport or degradation. The material component analysis developed here naturally captures the effect of time-dependent changes of ECM composition on the deformation and internal stress states of the ECM. For example, it is shown that increased synthesis of aggrecan by chondrocytes embedded within a decellularized cartilage matrix initially devoid of aggrecan results in osmotic expansion of the newly synthesized proteoglycan matrix and tension within the structural collagen network. Specifically, we predict that the collagen network experiences a tensile strain, with a maximum of ~2% at the fixed base of the cartilage. The analysis of an example problem demonstrates the temporal and spatial evolution of the stresses and strains in each component of a self-equilibrating composite tissue construct, and the role played by the flux of water through the tissue.

Keywords

cartilage; mathematical model; multi-phase; depth-dependent; osmotic swelling; tissue construct

1. Introduction

The functional role of articular cartilage is to facilitate smooth low-friction articulation and load transmission in diarthrodial joints. Articular cartilage is a multicomponent tissue (Heinegård, 2009) with spatially varying properties (Schinagl *et al.*, 1997). Early attempts at biomechanical descriptions of cartilage relied on modelling the tissue as a viscoelastic material (e.g. Coletti *et al.*, 1972; Hayes and Mockros, 1971). However, simple viscoelastic models could not fully represent the complex behaviour of the tissue (Mow *et al.*, 1980). Interaction between the tissue's extracellular matrix (ECM) and interstitial fluid were key to replicating many experimental findings, and any modelling framework needs to take into

*Correspondence to: D. W. Smith, Engineering Computational Biology Group, School of Computer Science and Software Engineering, University of Western Australia, 35 Stirling Highway, Crawley, WA 6009, Australia. david.smith@uwa.edu.au.

Conflict of interest The authors declare no conflicts of interest.

account these interactions. Poroelastic models of varying complexity do capture such interactions and are essential to understanding the mechanical behaviour of cartilage. Poroelastic models have physiologically meaningful parameters, such as tissue hydraulic permeability, porosity and matrix (visco)elasticity, that can be experimentally measured (Biot, 1962; Mow *et al.*, 1984). As a result, poroelastic models have become the norm for cartilage modelling. One of the most influential early models of cartilage mechanics was proposed by Mow *et al.* (1980). This `biphasic' model represented the tissue matrix as a solid phase saturated by water – the fluid phase; the solid phase is represented as a linear elastic material, and inhomogeneity of the solid and fluid phases can be included. More recently this biphasic framework has been extended to include orthotropic material properties (Korhonen *et al.*, 2003; Soulhat *et al.*, 1999). Wilson *et al.* (2004) investigated the stress in the collagen network using a biphasic swelling model that is reinforced with collagen fibrils, and analysed example problems using the finite element method. So-called triphasic and multiphasic models of cartilage also include the effects of electrolyte ions, in addition to the solid and fluid phases. These models address the dynamics of tissue swelling pressure and swelling strain associated with osmotic and electrochemical properties of the fluid and solutes (Eisenberg and Grodzinsky, 1987; Huyghe and Janssen, 1997; Lai *et al.*, 1991; Lu *et al.*, 2004). However, these previous models do not take into account the `turnover' of ECM molecules.

Articular cartilage is a dynamic tissue, with synthesis, degradation and transport of various ECM components all occurring simultaneously (Hascall *et al.*, 1990). Chondrocytes produce hundreds of extracellular and intracellular macromolecules (Heinegård, 2009), the two main load-bearing constituents being type II collagen and the proteoglycan aggrecan. Type II collagen fibrils are actually a heteropolymeric complex of types II, IX and XI molecules that polymerize into fibrils (Eyre *et al.*, 2006). Aggrecan is composed of a ~300 kDa core protein to which are connected ~100 chondroitin sulphate (CS) and, in some species, keratin sulphate (KS) glycosaminoglycan (GAG) chains (Ng *et al.*, 2003). Aggrecan associates non-covalently with hyaluronic acid (HA, hyaluronan) and the ~45 kDa link glycoprotein to form high molecular weight aggregates (> 200 MDa), which form a densely packed, hydrated gel enmeshed within the network of reinforcing collagen fibrils. Electrostatic repulsion and osmotic interaction forces associated primarily with the highly negatively charged CS GAGs develop a high swelling pressure resisted by the collagen network, and provide > 50% of the equilibrium compressive modulus of cartilage (Buschmann and Grodzinsky, 1995; Maroudas, 1979). Aggrecans are continuously synthesized by chondrocytes and degraded by proteases (aggrecanases; Nagase and Kashiwagi, 2003), whose activity is also mediated by the chondrocytes and other cells in diseased joints. Aggrecan and other ECM degradation products are continuously lost from the tissue into the synovial space. The spatially dependent mechanical properties of the tissue result from the non-uniform concentrations of aggrecans, collagen fibres and other matrix molecules.

In this paper we attempt to capture the dynamic mechanical equilibrium in articular cartilage, using an extensible modelling framework that separately accounts for each of the primary biomechanically functional matrix constituents of cartilage. Our goals are two-fold: (a) to develop a mathematical framework for biomechanical and biochemical modelling of cartilage (and constructs) turnover that can be adapted to various analysis needs; and (b) to illustrate the utility of this general mathematical framework by a simplified computational model of osmotic swelling.

2. Methods

2.1. General approach

Previously, DiMicco and Sah (2003) developed a continuum model to describe the relationship between spatially varying matrix concentrations and the processes of matrix formation, binding, degradation and molecular transport within and from the cartilage tissue. We extend this approach by incorporating such transport issues into a fully developed poromechanics treatment of the tissue. We also include the transport of many different types of solutes, including growth factors, nutrients and inflammatory molecules as required. By taking this approach, we foresee that we will be able to gain new insights into the `internal workings' of cartilage and so have a tool to answer new questions about the tissue; e.g. what is the predicted spatial distribution of cartilage components within the tissue, what is the distribution of half-lives of cartilage components in the tissue, and how long would it take for cartilage tissue constructs to achieve designed specified material properties? By modelling the components of cartilage, we have a means for understanding the development of the tissue and the sensitivity of the tissue to variations of each tissue component. This should enable us to better understand the tissue and the couplings that enable homeostasis, or facilitate tissue degradation or tissue regeneration.

We adopt a general continuum multicomponent model of cartilage, one that may be made as simple or as complex as experimental knowledge or a particular application requires. For example, the action of regulatory factors that control the synthesis and turnover of aggrecan, such as the IGF-1, TGFβ, IL-1β and TNFα systems can be incorporated to model ECM synthesis and degradation in a spatially dependent manner (Saha and Kohles, 2012; Zhang *et al.*, 2007). The distribution of ECM components will alter the transport and mechanical properties, which in turn alter the component distribution. Moreover, the distribution of these regulatory factors will be influenced by advection and diffusion, which are in turn dependent on the material properties of the cartilage. Strain- and strain rate-dependent physiological changes can also be introduced if required.

We illustrate the application of the proposed model, using the example of a devitalized tissue filling with aggrecan produced by chondrocytes seeded into the construct. We simplify our general model to a 'minimalist' model involving just three individual phases. Even this minimalist model of cartilage is relatively complex, requiring three partial differential equations and 15 material parameters. The model is run until final tissue equilibrium is reached between the collagen network, the water and the production and loss of aggrecan. Predictions of the depth-dependent aggrecan concentration and compressive modulus made by the calibrated model are compared with the experimental work of Klein *et al.* (2007). At steady state the model demonstrates its capability by being able to reproduce the experimentally observed properties for newborn calf cartilage. That is, it can reproduce the aggrecan distribution in newborn calf cartilage, measured cartilage compressive stiffness. The model is also able to predict the variable strain distribution throughout the collagen, and provide valuable insights into the dominant tissue processes that operate on different time scales.

2.2. Cartilage tissue and construct model: cells and ECM

Cartilage ECM or tissue constructs may be generally approximated as having three principal biomechanically functional components: (a) a structural network (for native cartilage the structural network is the collagen network, while in a tissue construct, prior to assembly of mature ECM, the initial structural network may be a `hydrogel', such as alginate, agarose or any number of scaffold materials); (b) aggrecans, made of GAG chains covalently attached to a core protein backbone (see Introduction); and (c) interstitial fluid (which is primarily

water with dissolved solutes). It is generally recognized that the various components of the ECM `turnover' on a variety of different time scales, ranging from minutes to decades. Once the tissue components of interest and the time scale for observation of the tissue system are known, it then becomes clearer which components of the ECM can be conveniently treated as `fixed' in time and which components should be treated as variable in time, and which components may be treated as solid-like vs fluid-like. In this way, a `general model' may be adjusted and particularized on the basis of problem requirements.

To capture the general behaviours of the ECM of interest in a `minimalist model', we may therefore start with five basic equations describing the movement, production and removal of cells, aggrecans (and related molecules), collagens (and related molecules), signalling molecules (e.g. growth factors, cytokines and chemokines) and of course the interstitial fluid (the principal component of cartilage by weight). Each component of this minimalist model is now considered in turn.

2.2.1. Structural network: collagens in the ECM—Here we consider the structural collagen network in native cartilage tissue, but the structural network in a decellularized tissue construct may be modelled in much the same way. However, there may be special features of the tissue construct which will require further components, as the scaffold likely degrades over time to be replaced by a new network of collagen. Thus, there may be a need to consider representing two structural networks within the early evolution of a tissue construct. Again, such a modelling choice depends on the time scale of observation; in our example problem below, we assume that the original collagen network remains intact.

The ECM of mature articular cartilage is about 60% collagen by dry weight (Maroudas, 1979). The collagen superfamily includes 28 collagen types expressed by > 43 distinct genes (Gordon and Hahn, 2010). The structural collagen network of the ECM is composed primarily of heteropolymeric fibrils containing types II, IX and XI, although additional collagens found in cartilage include types III, VI, X, XII, XIII and XIV (Eyre *et al.*, 2006). While fetal/newborn cartilage contains approximately 75% type II, 10% type IX and 10% type XI, adult cartilage contains up to 90% type II, 1% type IX, 3% type XI and up to 10% type III collagen (% of total collagen) (Eyre *et al.*, 2006). Collagen turnover in human articular cartilage is exceptionally slow, with a half-life estimated to be over 100 years (Verzijl *et al.*, 2000). Depending on need, all the equations for turnover of all relevant collagen types may be included; however, for our minimalist model developed here, the collagen network may be represented by three equations: (a) one for newly synthesized collagen molecules; (b) one for the structural collagen network (type II/IX/XI fibrils); and (c) one for degraded collagen. That is:

$$\frac{\partial c_{col,i}}{\partial t} = \nabla \cdot \left[D_{col,i} \nabla c_{col,i} - \mathbf{v}_{\mathrm{col,i}} c_{col,i} \right] + R_{col,i} \quad (1)$$

where the subscript col,*i* indicates the *i*th collagen constituent, with $i = 1$ for the newly synthesized collagen, $i = 2$ for the structural network and $i = 3$ for the degraded collagen. In equation (1) we might expect that the structural network form of collagen is unable to diffuse (i.e. $D_{\mathrm{col},2} = 0$). We might also expect that the advective velocity of the newly synthesized and degraded collagen will be a sum of the structural network collagen velocity $v_{\mathrm{col},2}$ and a contribution from the interstitial fluid velocity v_{f}. The collagen source/sink term $R_{\mathrm{col,i}}$ can be resolved into expressions for production and loss. This simplest case is:

$$R_{col,1}=k_{col,1}c_{cell}-k_{col,12}c_{col,1}$$
$$R_{col,2}=k_{col,12}c_{col,1}-k_{col,23}c_{col,2} \quad (2)$$
$$R_{col,3}=k_{col,23}c_{col,2}-k_{col,3}c_{col,3}$$

where $k_{col,1}$ is the production rate of $c_{col,1}$ per cell (units of `per time per cell'), $k_{col,3}$ is the degradation rate of $c_{col,3}$ (units of `per time') and $k_{col,12}$ and $k_{col,23}$ describe the rate of transition between the three forms of collagen (units of `per time'). In normal healthy cartilage, we might expect that the primary loss of proteolytically degraded collagen from cartilage is diffusion out through the cartilage/synovial surface, and so $k_{col,3}$ could be negligible. As chondrocytes can alter their collagen production rate $k_{col,1}$ or produce various enzymes to modify the rates of transition between these various states, in general these model rate parameters are not constant, but are likely to vary over time in a coordinated manner, according to regulatory systems controlling tissue homeostasis. Indeed, later we will give an example in which we assume that a proportional control system is operating to maintain collagen concentration at a set point.

Again, for simplicity, a generalized momentum balance equation for collagen is represented here:

$$\nabla \cdot \sigma^{\mathbf{col},i}+\sum_{\substack{j=1 \\ i\neq j}}^{N}\mathbf{F}^{\mathbf{j},\mathrm{col},\mathbf{i}}=\mathbf{0} \quad (3)$$

where *j* refers to all *N* primary components of the cartilage (i.e. cells, fluid, collagen types, aggrecan types). The osmotically-induced volume straining of the collagen network, as aggrecan concentration changes following aggrecan synthesis, may be introduced through the momentum flux exchange between the aggrecan and the collagen.

A suitable non-linear elastic model for the collagen network deformation may be chosen (e.g. one that is much stiffer in tension than compression), and again the elasticity tensor may be time dependent, as the size and complexity of the collagen network responds to deposition of newly synthesized collagens or degradative proteases. A suitable simple stress–strain constitutive relationship is:

$$\sigma_{ij}^{col,i}=D_{ijkl}^{col,i}e_{kl}^{col,i} \quad (4)$$

where $e_{kl}^{col.i}$ is the small strain tensor for the collagen network and is a non-linear, time-dependent 6 × 6 elasticity matrix, comprising values of Young's moduli and Poisson's ratio for the structural collagen network. For the simplest isotropic structural network, this 6 × 6 matrix reduces to just two material constants in each of tension and compression, Young's modulus and Poisson's ratio.

2.2.2. GAGs and proteoglycans in the ECM—The ECM of mature articular cartilage contains about 35% proteoglycans by dry weight (Maroudas, 1979). The proteoglycan (PG) superfamily includes large and small extracellular macromolecules as well as specialized pericellular and membrane-bound constituents (Heinegård, 2009). Aggrecan is the primary structural, large aggregating PG in cartilage pericellular and extracellular matrix, having a concentration and molecular structure that varies with human/animal age, cartilage depth, location along a joint surface and radial distance from the cell. Members of the small leucine-rich PG subfamily (SLRPs), e.g. biglycan, decorin and fibromodulin, can bind to collagen fibrils and thereby regulate collagen fibril diameter and network self-assembly. All these members of the PG family are defined by: (a) the amino acid sequence of their core

proteins; and (b) the glycosylation of the core protein (elongation and sulphation of GAG chains initiated at specific amino acid residues of the core) that takes place within the cell during PG synthesis. Chondroitin sulphate GAGs (20–40 nm) are the main biomechanically functional GAG chains along the aggrecan core protein, although there are also keratin sulphate chains (~ 10 nm) present in selected regions of aggrecan. Additional members of the PG family, along with many other ECM proteins, play an important role as binding partners between biomechanically structural matrix elements to assemble and maintain the integrity of the ECM. Indeed, together with tissue responses to mechanical loading, such biochemical interactions are the foundation for the feedback processes that maintain tissue homeostasis. Because the feedback processes within a tissue span many functional levels and are often redundant, interactions are often observed to occur between seemingly disparate tissue components, which may be crucial to developing a realistic representation of tissue behaviour.

For our minimalist model of aggrecan turnover, we proceed as we did for the collagen model. Three different equations are required, including mobile newly synthesized aggrecans, less mobile aggrecans that are bound to hyaluronan (a binding motif stabilized by the ~45 kDa `link' protein), and mobile degraded aggrecan fragments, generated primarily by the aggrecanases. For simplicity, we write a general aggrecan equation that would be part of a model of aggrecan turnover:

$$\frac{\partial c_{agg,i}}{\partial t} = \nabla \cdot \left[D_{agg,i} \nabla c_{agg,i} - \mathbf{v}_{\mathrm{agg},\mathbf{i}} c_{agg,i} \right] + R_{agg,i} \quad (5)$$

In equation (5), $i = 1$ corresponds to newly synthesized aggrecan, $i = 2$ for the much less mobile aggrecan aggregate (that may be physically enmeshed within the collagen network and/or connected to it via ECM linker molecules) and $i = 3$ is degraded aggrecan. While aggrecan fragments are smaller than newly synthesized 'full-length' aggrecan, their diffusion coefficients would likely be orders of magnitude higher than aggregated aggrecan (DiMicco and Sah, 2003; Hascall *et al.*, 1990). Aggrecan species may advect with the structural collagen network, and may advect independent from the collagen network under certain conditions. As for the collagen, we might expect the following as a simple model for the production of aggrecan and its transition through the various forms of aggrecan considered here:

$$\begin{aligned} R_{agg,1} &= k_{agg,1} c_{cell} - k_{agg,12} c_{agg,1} \\ R_{agg,2} &= k_{agg,12} c_{Agg,1} - k_{agg,23} c_{agg,2} \\ R_{agg,3} &= k_{agg,23} c_{agg,2} - k_{agg,3} c_{agg,3} \end{aligned} \quad (6)$$

where $k_{\mathrm{agg},1}$ is the production rate of $c_{\mathrm{agg},1}$ per cell (units of `per time per cell'), $k_{\mathrm{agg},3}$ is the degradation rate of $c_{\mathrm{agg},3}$ (units of `per time') and $k_{\mathrm{agg},12}$ and $k_{\mathrm{agg},23}$ describe the rate of transition between the three forms of aggrecan (units of `per time'). As with the production and degradation model for collagen [equation (2)], the various rate parameters in equation (6) are generally not constant. Instead they are expected to vary as the chondrocytes respond to their local microenvironment (mechanical and chemical stimuli) by changing production and degradation rates of the various aggrecans. When the degradation rate of aggrecan is small, e.g. in young, normal healthy cartilage compared to adult osteoarthritis (OA) cartilage, and loss from the tissue of newly synthesized (full-length) aggrecan by diffusion may be more relevant, one may choose to neglect $k_{\mathrm{agg},3}$.

The momentum balance for aggrecan may be written as:

$$\nabla \cdot \sigma^{\mathbf{agg},i} + \sum_{\substack{j=1 \\ i \neq j}}^{N} \mathbf{F}^{j,\mathrm{agg},i} = \mathbf{0} \quad (7)$$

where **j** refers to all **N** primary components of the cartilage (i.e. cells, fluid, collagen types, aggrecan types). A suitable non-linear elastic model for aggrecan deformation may be chosen, which again may be time dependent as the cell responds to local microenvironmental stimuli, such as strain, growth factors and cytokines, and so produces new aggrecan molecules (and proteins that provide the structural support for the aggrecan molecules).

Load deformation may be introduced through a simple stress–strain constitutive relationship, viz:

$$\sigma_{ij}^{agg,i} = D_{ijkl}^{agg,i} e_{kl}^{agg,i} \quad (8)$$

where $e_{kl}^{agg,i}$ is the small strain tensor and $D_{ijkl}^{agg,i}$ is a non-linear, time-dependent elasticity matrix, comprising values derived from osmotic moduli (viz. $K^{os} = c^{agg} \frac{\partial \prod^{agg}}{\partial c^{agg}}$, see Section 2.2.7.) and Poisson's ratio. Again, for isotropic materials experiencing small changes, this 6 × 6 matrix reduces to just two material constants, Young's modulus and Poisson's ratio.

2.2.3. Chondrocytes—Chondrocytes occupy about 2–10% of the volume of articular cartilage, depending on the age of the tissue (Gilmore and Palfrey, 1988). While chondrocytes in normal, healthy cartilage appear to demonstrate little or no proliferation, cartilage injury and osteoarthritis (Dreier, 2010) can induce cell proliferation in affected regions. The time scale of observation of such events is critical to definitive conclusions regarding proliferation. In a tissue construct, chondrocytes can undergo random movement (migration), which can be modelled as a diffusion process. In both native cartilage and the tissue construct there may be directed cell movement, which may be modelled as an advection movement. That is:

$$\frac{\partial c_{cell}}{\partial t} = \nabla \cdot \left(D_{cell} \nabla c_{cell} - \mathbf{v}_{\mathbf{cell}} c_{cell} \right) + R_{cell} \quad (9)$$

The `advection' velocity of chondrocytes, v_{cell}, can be thought of as the sum of the chondrocyte directed migration velocity (e.g. chemoattractant-induced migration) together with movement of the collagen structural network (within which the chondrocytes are located), $v_{\mathrm{col},2}$. It is known, for example, that cell production of aggrecan can lead to local deformation of the collagen network in native tissue and engineered constructs. Indeed, the aggrecans serve to `inflate' the structural network, and so result in a self-equilibrating stress state, with the structural network in tension and the aggrecan molecules in compression. The simplest model for chondrocyte production/loss is:

$$R_{cell} = \left(k_{cell} - a_{cell} \right) c_{cell} \quad (10)$$

where k_{cell} is the rate of production of new chondrocytes (units of `per time per cell') and $a_{\mathrm{cell}}$ is the rate of chondrocyte apoptosis/necrosis (units of `per time per cell'). These rates will vary in time in response to the microenvironment of chondrocytes. For example, chondrocytes near a focal defect or in a region of altered ECM caused by early OA may undergo migration and proliferative activities in an attempt to repair local ECM (Dreier,

2010; Hunziker and Rosenberg, 1996). The rate of chondrocyte apoptosis is likely to change, too, depending on environmental conditions (e.g. when large mechanical strains are encountered, particularly in the superficial zone of native cartilage, and in cell-seeded hydrogel subject to joint articulation; Grogan *et al.*, 2012; Kisiday *et al.*, 2004).

We note that chondrocyte migration through the ECM is likely to be very slow under normal physiological conditions, making their migration difficult to observe in most experimental systems of native cartilage. For this reason, it is only recently that researchers have suggested that chondrocytes may migrate through cartilage tissue under normal physiological conditions (e.g. Simkin, 2008). However, it is observed that chondrocytes migrate in vitro (Morales, 2007) and migrate in vivo sufficiently quickly to be observed on a time scale of weeks when the amount of ECM matrix is low, as may occur in injury, repair or disease states such as OA. Additionally, within hydrogel constructs, migration of chondrocytes (and stem cells undergoing chondrogenesis) has been well documented, and depends to a great extent on the mechanical and chemical properties of the scaffold (Ng *et al.*, 2012).

We may also write a momentum balance equation for the chondrocytes, but whether or not this is required depends on the length scale of the chondrocyte relative to the characteristic length scale for the problem of interest. For example, as a chondrocyte is 10–15 μm in diameter, it may useful to include a momentum balance equation for the chondrocytes for problem length scales up to about 100–150 μm. For length scales above several hundred mm, the chondrocyte properties may be reasonably included within ECM properties, and for this reason explicit momentum equations for the chondrocytes may not be required.

In any case, based on the previous momentum balance equation, the momentum balance for chondrocytes may be written as:

$$\nabla \cdot \sigma^{cell} + \sum_{i=1}^{N-1} \mathbf{F}^{i,cell} = \mathbf{0} \quad (11)$$

where i refers to all N primary components of the cartilage (i.e. fluid, collagen types, aggrecan types) not including cells. A suitable non-linear elastic model for cell deformation may be chosen, which may include time-dependent parameters to reflect the cellular responses (e.g. reorganization of cell cytoskeleton) to local microenvironmental stimuli (such as strain, growth factors and cytokines). However, there may be osmotically-induced volume strains in the cell due to changing intracellular proteoglycan concentrations and ion pump responses. This osmotically induced cell deformation may be included in the model in a way that is analogous to a temperature change in thermoelasticity. In other words, the osmotically induced cell deformation may be introduced through a non-linear stress–strain constitutive relationship, viz:

$$\sigma_{ij}^{cell} = D_{ijkl}^{cell} \left(e_{kl}^{cell} - \delta_{kl} \lambda^{cell} \Delta \prod^{cell} \right) \quad (12)$$

where e_{kl}^{cell} is the small strain tensor and D_{ijkl}^{cell} is a 6 × 6 elasticity matrix, comprising values of Young's modulus and Poisson's ratio for the chondrocyte, is the coefficient of osmotic expansion and is the osmotic pressure change relative to a reference osmotic pressure for the cell. The elasticity tensor may be directional, non-linear and different in compression and tension, and these cell properties may change as cells respond to changes in the local microenvironment. In the simplest model of an isotropic cell, this 6 × 6 matrix reduces to just two material constants, Young's modulus and Poisson's ratio.

2.2.4. Transport of solute in the ECM—Solute molecules of possible interest here include oxygen, nutrients, waste products from chondrocytes, growth factors such as IGF-1, cytokines such as IL-1 and potential therapeutic molecules (small-chemical and large-biologics) to address clinical issues of cartilage repair and OA. The movement of the ith solute within the ECM can be with the fluid or with one of the other ECM components. Movement with the *i*th solute is represented by:

$$\frac{\partial c_i}{\partial t} = \nabla \cdot \left[D_i \nabla c_i - \mathbf{v_f} c_i \right] + R_i \quad (13)$$

where $v_d = v_f - v_{agg}$ is the Darcy flow of water (note that this representation of the Darcy velocity presupposes that the principal drag on water arises from the GAG molecules – see later discussion on component interactions and that solutes are primarily transported with the fluid). Movement of solute with another phase would be described by:

$$\frac{\partial c_i}{\partial t} = \nabla \cdot \left[-\mathbf{v} c_i \right] + R_i \quad (14)$$

where it has been assumed that diffusion in these other ECM components is negligible. The advective velocity *v* is the velocity of the relevant ECM component within which the solute is being transported. Exactly which molecules are included in an analysis depends on the problem and the application. There is no separate momentum balance equation written for molecular transport.

2.2.5. Transport of water in the ECM—The ECM in mature cartilage is approximately 75% water by weight (Comper, 1991). Because the pressures experienced in tissues under physiological conditions are relatively low, water and other components may be treated as incompressible. If it is assumed that any component is not influenced by others in the mixture (but noting this assumption may be relaxed as required), then using the incremental volume constraint equations leads to:

$$\frac{de_v^{col}}{dt} = -\nabla \cdot \mathbf{v_d} + \sum \nabla \cdot f_{vol}^n + \sum R_{vol}^n \quad (15)$$

where the elastic volumetric strain of the collagen network is e_v, v_d is the Darcy velocity of water, $f_{\mathrm{vol}}^{\mathrm{n}}$ are the net volume fluxes into the REV and $R_{\mathrm{vol}}^{\mathrm{n}}$ is the volume source of sink, for components other than water and structural collagen. The above equation is of critical importance to porous media mechanics, as it couples the solid phase deformation to fluid phase movement, and is responsible for characteristic poroelastic behaviours such as the Mandel–Cryer effect (Cryer, 1963).

The movement of water is induced by a gradient in the chemical potential, μ^{w}, of the water:

$$\mu^w = \sum_{n=1}^{3} \frac{tr\left(\sigma^{\mathbf{agg},i}\right)}{3} - \prod^{aggtot} \quad (16)$$

where μ^{w} is equal to the `hydrostatic total stress' carried by all the aggrecans $\left(\sum_{i=1}^{3} tr\left(\sigma^{\mathrm{agg},i}\right) = tr\left(\sigma^{\mathrm{s}}\right) - \sum_{i=1}^{3} tr\left(\sigma^{col,i}\right)\right)$ minus the `osmotic pressure' (Π) generated by the total aggrecan concentration; see Comper (1991) for definition of the osmotic pressure, which is identical to the chemical potential of the aggrecan. At equilibrium the chemical potential of the water is zero, and this occurs when $\sum_{n=1}^{3} \frac{tr\left(\sigma^{\mathbf{agg},i}\right)}{3} = \prod^{aggtot}$.

implicit assumption here is that the osmotic pressure generated by all other components in the material is relatively small compared to that of the aggrecan (which is taken to include the counter-ions required for electroneutrality of the aggrecan molecules), and that the background electrolyte concentration is held constant.

The movement of water in porous materials is most usually represented as a so-called `Darcy flow'. Darcy's law is a minimalist form of the momentum balance equation for water. Darcy's law states that the Darcy flow is proportional to the gradient of the chemical potential of the water, with the proportionality constant referred to as the hydraulic conductivity (k) for the material, viz:

$$\begin{aligned}\mathbf{v_d} &= (\mathbf{v}_f - \mathbf{v_{agg}}) = -k\nabla\mu \\ &= -k\nabla\left(\frac{tr(\sigma^{\mathbf{agg}})}{3} - \prod^{aggtot}\right)\end{aligned} \quad (17)$$

Combining equations (15) and (17) leads to:

$$\frac{\partial e_v^{col}}{\partial t} = \nabla\cdot\left[k\nabla\left(\frac{tr\left(\sigma^{\mathbf{agg}}\right)}{3} - \prod^{aggtot}\right)\right] + \sum\nabla\cdot f_{vol}^n + \sum R_{vol}^n \quad (18)$$

2.2.6. Momentum interactions between material components—Until now we have not discussed the momentum interactions between the primary cartilage components, specifically as they relate to terms appearing in equations (3, 7 and 11). We now turn our attention to these momentum interactions. If the primary components of cartilage are taken to be cells, structural collagen, the three types of aggrecan (newly synthesized aggrecan, `fixed' or aggregated aggrecan and degraded aggrecan) and water, then there are six separate components. Theoretically, each component may interact with the other and exchange momentum, so there may be $C_2^6 = 15$ possible combinations of momentum interaction between the components. But let us assume that it is the gradient of the `total' aggrecan osmotic pressure that interacts with the collagen (and from a momentum perspective, all components are identical in contributing to the aggrecan osmotic pressure). Then the number of potentially significant momentum interactions is reduced to four components.

Let us now assume the drag of the aggrecan and water on the cells is zero. Let us further assume the drag force of the water on the structural collagen network is negligible compared to the drag resistance offered by the aggrecan GAG chains. This leaves three remaining momentum interactions unaccounted for.

Let us assume the principal drag force of the aggrecan on the structural collagen network is the gradient of the total aggrecan osmotic pressure. Then the body force acting on the mobile aggrecan is given by:

$$\mathbf{F}_i^{\mathbf{colGAG}} = \nabla\sum_{n=1}^{Naggs}\prod^n = \nabla\prod^{tot} \quad (19)$$

and, as action and reaction are equal and opposite:

$$f_i^{colGAG} + f_i^{GAGcol} = \mathbf{0} \quad (20)$$

Also, we have assumed previously that the principal drag force for the water is the total aggrecan concentration, so that:

$$f_i^{waterGAG} = \nabla \cdot \left(\sum_{n=1}^{Naggs} \frac{tr\left(\sigma^{aggn}\right)}{3} - \prod^{aggtot} \right) \quad (21)$$

and, again as action and reaction are equal and opposite:

$$f_i^{waterGAG} + f^{GAGwater} = 0 \quad (22)$$

This accounts for all the component momentum interactions.

2.2.7. Osmotic potential of aggrecan—The osmotic pressure of the aggrecans in the ECM is of critical importance of the normal function and behaviour of the cartilage tissue, so this is discussed in more detail here. The osmotic pressure is given by Bathe *et al.* (2005) as:

$$\prod^{agg} = \alpha_1 c^{agg} + \alpha_2 (c^{agg})^2 + \alpha_3 (c^{agg})^3 \quad (23)$$

where c^{agg} is the concentration of aggrecan in moles, $\alpha_1 = RT$ is the product of the universal gas constant and absolute temperature, and $\alpha_{2,3}$ are the first and second virial coefficients.

It turns out that the virial coefficients are important and in fact play the primary role in generating osmotic pressures at physiological levels of aggrecan concentration found in cartilage (Bathe *et al.*, 2005; Comper, 1991). This is due to the fact that the aggrecan GAG chains have a high density of ionized fixed charge groups (carboxyl and sulphate) under physiological conditions, and the counter-ions associated with these fixed charges make the most significant contribution to the osmotic pressure of an aggrecan polymer solution. A reference condition (e.g. the normal physiological state) for the osmotic pressure equation needs to be specified because the virial coefficients are strong functions of: (a) the relative proportions of component molecules; (b) the pH; (c) the ionic strength and composition of the bathing fluid and; (d) temperature. Having defined a reference state, an incremental change in the osmotic pressure from that reference state is given by:

$$d\prod^{agg} = \sum_{i=1}^{n} \frac{\partial \prod^{agg}}{\partial \alpha_n} d\alpha_n + \frac{\partial \prod^{agg}}{\partial c^{agg}} dc^{agg} \quad (24)$$

However, because the volume of the tissue may also change (say due to a deformation of the collagen network), then a change in aggrecan concentration may occur either by the addition of new aggrecan molecules at constant volume or by a change in volume of the solution (or tissue), and so:

$$dc^{agg} = d\left(\frac{moles}{volume}\right) = \frac{dm^{agg}}{V} - c^{agg} de_v^{col,2} \quad (25)$$

where $e_v^{col,2}$ is the reference volume strain. Taking into account volume change of the tissue in the incremental osmotic equation leads to:

$$d\prod^{agg} = \sum_{i=1}^{n} \frac{\partial \prod^{agg}}{\partial \alpha_n} d\alpha_n + \frac{\partial \prod^{agg}}{\partial c^{agg}} \left(dc^{agg} - c^{agg} de_v^{col,2} \right) \quad (26)$$

which is sometimes written as:

$$d\prod^{agg}=\sum_{i=1}^{n}\frac{\partial\prod^{agg}}{\partial\alpha_n}d\alpha_n+\frac{\partial\prod^{agg}}{\partial c^{agg}}dc^{agg}-K^{os}de_v^{col,2} \quad (27)$$

where $K^{os}=c^{agg}\frac{\partial\prod^{agg}}{\partial c^{agg}}$ is called the `osmotic modulus' (Horkay *et al.*, 2008).

As noted above, a change in the virial coefficients may result from a change in the composition of the aggrecan polymer mixture, from a change in the ionic strength of the bathing solution, from a change in the charge density on the aggrecan molecules (e.g. from a change in pH of the tissue) and from a change in temperature. We see that the osmotic pressure may be viewed as a complex hypersurface in a multidimensional state space. The response of the osmotic pressure to changes in a variety of variables can be explored empirically, and the hypersurface approximated in variety of different ways depending on the purpose of the empirical investigation.

For example, if the effects of a change in background ionic strength of the bathing solution (BIS), a change in pH of the bathing solution, a change in composition of the mixture of polymers [e.g. say due to a change in hyaluronic acid (HA) and linker protein concentration], a change in concentration of aggrecan concentration at constant volume and volume deformations are to be investigated empirically, then equation (27) above may be approximated by:

$$d\prod^{agg}=\sum_{i=1}^{n}\frac{\partial\prod^{agg}}{\partial BIS}\frac{\partial BIS}{\partial\alpha_n}d\alpha_n+\sum_{i=1}^{n}\frac{\partial\prod^{agg}}{\partial pH}\frac{\partial pH}{\partial\alpha_n}d\alpha_n+\sum_{i=1}^{n}\frac{\partial\prod^{agg}}{\partial HA}\frac{\partial HA}{\partial\alpha_n}d\alpha_n+\frac{\partial\prod^{agg}}{\partial c^{agg}}dc^{agg}-K^{os}de_v^{col,2} \quad (28)$$

or, in terms of more experimentally accessible variables:

$$d\prod^{agg}=\frac{\partial\prod^{agg}}{\partial BIS}dBIS+\frac{\partial\prod^{agg}}{\partial pH}dpH+\frac{\partial\prod^{agg}}{\partial HA}dHA+\frac{\partial\prod^{agg}}{\partial c^{agg}}dc^{agg}-K^{os}de_v^{col,2} \quad (29)$$

If these variables are now changed independently of one another, then the material parameters may be identified. For example, dividing through by the volume strain, we find:

$$\frac{d\prod^{agg}}{de_v^{col,2}}=\frac{\partial\prod^{agg}}{\partial BIS}\frac{dBIS}{de_v^{col,2}}+\frac{\partial\prod^{agg}}{\partial pH}\frac{dPH}{de_v^{col,2}}+\frac{\partial\prod^{agg}}{\partial HA}\frac{dHA}{de_v^{col,2}}dHA+\frac{\partial\prod^{agg}}{\partial c^{agg}}\frac{dc^{agg}}{de_v^{col,2}}-K^{os} \quad (30)$$

and, assuming the volume strain is independent of the other variables, then:

$$\frac{d\prod^{agg}}{de_v}=-K^{os} \quad (31)$$

As a change in stress with respect to a change in strain is referred to as a `modulus', this explains why $K^{os}=c^{agg}\frac{\partial\prod^{agg}}{\partial c^{agg}}$ is referred to as the `osmotic modulus' (Horkay *et al.*, 2008).

Horkay *et al.* (2008) experimentally examined the effect of change in composition of the polymer mixture on osmotic pressure, and found that the addition of hyaluronic acid (HA) and linker protein to a GAG polymer solutions to form a aggrecan polymer solution results in a substantial reduction (about 30%) of osmotic pressure at low aggrecan concentrations (50 mg aggrecan/ml). However, it was found that this reduction in osmotic pressure becomes smaller as aggrecan concentration increases, so that at physiological concentrations

of aggrecan, the effect of HA on the osmotic pressure is minimal. However, Horkay *et al.* (2008) also note that the osmotic modulus is considerably increased by the presence of HA at physiological concentrations of aggrecan.

If the experimental variables are believed not to be independent of one another, or their values are difficult to independently control experimentally, then it may be appropriate to just measure the osmotic modulus for specific environmental conditions and not attempt to link this measured value to underlying changes in state variables.

Another approach is to use various theories of polymer behaviour to understand the osmotic pressure response of the polymer mixture. For example, Donnan equilibrium theory (which predicts ion redistributions in response to the presence of immobile or `fixed' charge) may be employed to estimate the difference in ion concentrations ($DIS = PIS - BIS$) between the polymer mixture (PIS) and the ionic strength of the bathing solution (BIS) as a function of charge density, the aim being to separate the component of osmotic pressure change due to change in ion distributions from that component of osmotic pressure due to the concentration of uncharged polymers c^{aggnull}. Assuming that these two effects are independent, a change in the osmotic pressure hypersurface is represented by:

$$d\prod^{agg} = \frac{\partial \prod^{agg}}{\partial DIS} dDIS + \frac{\partial \prod^{agg}}{\partial c^{aggnull}} dc^{aggnull} \quad (32)$$

Experimental and theoretical investigations have shown that the Donnan theory consistently overestimates the effect of ion redistributions on the osmotic pressure, as the Donnan theory assumes that the ion distribution in the polymer solution is uniform, when in fact at the microscale the ion distribution is non-uniform. To take into account the non-uniform microscale ion distribution, a microstructural model of the Poisson–Boltzmann (PB) distribution of ions within a unit cell may be employed, and this proves to be much more effective representation of osmotic pressure induced by the changes in ion redistribution (Buschmann and Grodzinsky, 1995).

2.3. Example: aggrecan production within a chondrocyte seeded collagen scaffold

A common process in tissue engineering is growing artificial tissue from cell-seeded scaffolds. In order to demonstrate the functionality of this modelling framework, we treat the case of a decellularized cartilage matrix (Ghanavi *et al.*, 2012) to be used as a construct for repair of cartilage defects, based on the strategy that, devoid of antigenic cell components, the remaining ECM has relatively low immunogenicity (Kang *et al.*, 2012). Such cartilage-derived scaffolds, initially devoid of cells and aggrecan, have been demonstrated to contain a fully intact collagen fibrillar network, thereby enabling the construct to have tensile behaviour near that of native cartilage tissue (Kheir *et al.*, 2011). Chondrocytes can be seeded into such constructs by a variety of methods (Gong *et al.*, 2011; Minehara *et al.*, 2011), with the ultimate goal of cell synthesis of aggrecan (and other non-collagenous proteins) so as to achieve cartilage-like depth-dependent aggrecan concentrations and associated compressive and osmotic swelling behaviour. Starting with an initially uniform density of seeded chondrocytes, we demonstrate the model's ability to predict spatial–temporal increases in osmotic expansion of the newly synthesized proteoglycan matrix, resulting in a further increase in tension within the structural collagen network (as reported by Gong *et al.*, 2011) that can thereby restrict proteoglycan and water movement. The analysis also demonstrates the temporal and spatial evolution of the stresses and strains in each component of the tissue construct.

For simplicity, i.e. consistent with a goal of using this simplified model to illustrate the application of the general cartilage model, the model starts with an isotropic collagen fibrillar network derived from decellularized cartilage, uniformly seeded with chondrocytes. The cells are assumed to synthesize and secrete aggrecan uniformly throughout the collagen network for the duration of the simulation. The simulation is run until a dynamic equilibrium between the concentrations and stresses of the collagen, aggrecan and water is reached. This simulation is able to demonstrate the interaction and relative movement of the collagen, aggrecan and fluid phases as well as the spatially varying stresses and strains developed throughout the depth of the collagen construct.

2.4. Reduced set of equations

For this minimalist model of the tissue construct, we identify three momentum balance equations and three constitutive relationships, one of each for the collagen network (which is assumed unchanged over the time period of the analysis), the newly synthesized aggrecan (represented by a spatially uniform source term in the model), and water.

The momentum balance equations are:

$$\nabla \cdot \sigma^{\mathrm{col}} + \sum F_i^{\mathrm{col}} = 0 \quad (33)$$

$$-\nabla \Pi^{\mathrm{agg}} + \sum F_i^{\mathrm{agg}} = 0 \quad (34)$$

$$-\nabla p^{w} + \sum F_i^{w} = 0 \quad (35)$$

The collagen, aggrecan, and fluid phases are denoted by superscripts, col, agg and w, respectively. The subscript *i* denotes the body force with respect to the other phases. For example, the total body force on the collagen, F^{col}, is the sum of the interaction of collagen with aggrecan, $F_{\mathrm{agg}}^{\mathrm{col}}$, and collagen with water, F_{w}^{col}. As all of the interaction forces between phases are equal and opposite (e.g. $F_{\mathrm{agg}}^{\mathrm{col}} = -F_{\mathrm{col}}^{\mathrm{agg}}$), summing the three momentum equations gives:

$$\nabla \cdot \sigma^{\mathrm{col}} - \nabla \Pi^{\mathrm{agg}} - \nabla p^{w} = 0 \quad (36)$$

The constitutive equation used here for modelling the collagen network is a bilinear modification to the simple linear elasticity equation, $\sigma^{\mathrm{col}} = E^{\mathrm{col}}/\epsilon^{\mathrm{col}}$, to account for a difference in stiffness of collagen under compression vs tension. A linear model is adequate for the small deformations considered here. In this elasticity equation ϵ^{col} represents the strain in the collagen and E^{col} represents the Young's modulus of the collagen. Here E^{col} is defined to be isotropic and stepwise linear, with $\epsilon^{\mathrm{col}} > 0$ in tension (E^{col} = 5MPa) and $\epsilon^{\mathrm{col}} < 0$ in compression (E^{col} = 0.5MPa; values in Table 1).

The volume constraint equation for the system is derived as follows. The volume change of a representative elementary volume (REV) is equivalent to the divergence of the volume flux (f_i^v) of the aggrecan and water, plus any volume source or sink terms (s_i^v):

$$\frac{\partial e_v}{\partial t} = -\nabla \cdot \sum_{i=1}^{2} f_i^v + \sum_{i=1}^{2} s_i^v \quad (37)$$

The collagen is treated as deformable but is not transported by diffusion or convection. For aggrecan and extracellular fluid, we propose that the volume flux is defined as:

$$f_i^v = n_i \left(v^i - v^{\text{ref}} \right) \quad (38)$$

where n_i is the volume fraction of phase i, v^i is the true velocity (with respect to spatial coordinates) and v^{ref} is the velocity of the reference phase. Collagen is defined to be the reference material, as it simplifies the definition of boundary conditions. We chose to define the interaction of the extracellular fluid with the aggrecan phase only, as the interaction with the collagen phase is small in comparison. We then rewrite the above equation for the fluid phase as:

$$f_w^v = n_w \left[(v^w - v^{\text{agg}}) + \left(v^{\text{agg}} - v^{\text{col}} \right) \right] \quad (39)$$

$$= v_{\text{darcy}}^w + \frac{n_w}{n_{\text{agg}}} v_{\text{darcy}}^{\text{agg}} \quad (40)$$

Using the constitutive relationships for water and aggrecan defined in equation (7):

$$f_w^v = -k^w \nabla p^w - \frac{n_w}{n_{\text{agg}}} k^{\text{agg}} \nabla p^{\text{agg}} \quad (41)$$

The permeabilities k^w and k^{agg} are non-linear functions of aggrecan concentration (refer to Table 1) and are a combination of the specific conductivity and viscosity of the respective materials. Combining the above equation with the Darcy expression for aggrecan gives our final volume constraint equation:

$$\frac{\partial e_v}{\partial t} = \nabla \cdot (k^w \nabla p^w) + \nabla \cdot \left[\left(1 + \frac{n_w}{n_{\text{agg}}} \right) (k^{\text{agg}} \nabla p^{\text{agg}} \right] + s_w^v + s_{\text{agg}}^v \quad (42)$$

We note that $p^{agg} = \Pi^{\text{agg}} + p^w$. The aggrecan volume source s_{agg}^v is derived from s_{agg}^M (the mass source as described below) using the partial specific volume of GAG 0.55 ml/g (compiled from Franzen and Heinegard, 1984; Luscombe and Phielps, 1967; Heinegard *et al.*, 1981). For the purposes of this example we assume that there are no significant volume sources or sinks for water.

We are also interested in modelling the molar concentration of aggrecan, as this determines the osmotic pressure in the tissue and the subsequent driving force for aggrecan movement. It is common in experimental protocols to measure the concentration of aggrecan in mg/ml instead of molar concentrations. This is because of the variability in the molecular weight of the aggrecan molecules. In this example we will calculate the aggrecan concentration in units of mg/ml. We again start with a balance equation:

$$\frac{\partial c_{\text{agg}}}{\partial t} = -\nabla \cdot f^M + s_{\text{agg}}^M \quad (43)$$

where c_{agg} is the concentration of aggrecan, (f^M) is the flux of the aggrecan and $\left(s_{\text{agg}}^M \right)$ is the net source term. If we assume that aggrecan is primarily advectively transported, we can

describe the aggrecan mass flux as $f^M = c^{agg} v^{agg}$. Substituting this mass flux relationship into equation (43) gives:

$$\frac{\partial c_{\mathrm{agg}}}{\partial t} = -\nabla \cdot \left[v^{\mathrm{agg}} c^{\mathrm{agg}} \right] + s^M_{\mathrm{agg}} \quad (44)$$

Note that (v^{agg}) can be expressed in terms of the known (v^{col}) as (v^{col}), again ($p^{agg} = \Pi^{agg} + p^w$), and thus the mass balance for the aggrecan becomes:

$$\frac{\partial c_{\mathrm{agg}}}{\partial t} = \nabla \cdot \left[\left(k^{\mathrm{agg}} \nabla \left(\Pi^{\mathrm{agg}} + p^w \right) - v^{\mathrm{col}} \right) c_{\mathrm{agg}} \right] + s^M_{\mathrm{agg}} \quad (45)$$

The osmotic pressure within cartilage is directly dependent on the aggrecan concentration. Using the concentration given by equation (45), we use the following relation to calculate the osmotic pressure (Bathe *et al.*, 2005):

$$\Pi^{\mathrm{agg}} = R.T \left(\alpha_1 c^{\mathrm{agg}} + \alpha_2 (c^{\mathrm{agg}})^2 + \alpha_3 (c^{\mathrm{agg}})^3 \right) \quad (46)$$

where R is the universal gas constant and (T) is the temperature (K). The constants (α_{1-3}) are the virial coefficients.

Equations (36, 42, 45 and 46) are our reduced set of equations that will be solved in this example problem. These equations are solved numerically using the commercial Finite Element Method solver Comsol Multiphysics v. 4.3. In Comsol we used the modules Solid Mechanics [equation (36)]; Darcy's Law [equation (42)]; Coefficient PDE [equations (45 and 46)] and default settings for discretization.

2.5. Problem geometry and boundary and initial conditions

We have chosen to solve the equations in a two-dimensional (2D) geometry (see Figure 1) to enable comparison with future 2D problems, but with boundary conditions which effectively make the the problem a one-dimensional (1D) problem, i.e. only variation with cartilage depth. Specifically, the geometry for the 2D cartilage construct is 1 mm deep 100 mm wide (refer to Figure 1). The base is impermeable and fixed in space, and both sides have roller boundary conditions (frictionless, without normal displacement). Only the top surface is permeable to water and aggrecan, and this surface has a water boundary pressure of 0 Pa. These boundary conditions are consistent with a section of cartilage in contact with an underlying bone (in native tissue) or an artificial support (in the case of cartilage constructs), surrounded to the sides by a similar matrix structure and exposed at the top surface to a solute bath or synovial joint.

Experimentally it is observed that aggrecan concentration varies with depth and is approximately 20–50% lower at the surface than in the middle or deep zones of normal immature cartilage (Klein *et al.*, 2007). This lower aggrecan concentration at the surface may be due to several factors, including differences in the biosynthetic activity of cells in the superficial zone (compared to those in deeper zones) as well as the time needed for newly synthesized aggrecan to bind with high affinity to hyaluronan to form aggregates (~12 h in immature cartilage; Sandy *et al.*, 1989) and, in the absence of such binding, the aggrecan monomer could more easily diffuse out of the tissue. Taken together, one modelling approach is to represent such phenomena as a transport resistance boundary condition at the surface. Here, we use a Robin boundary condition and with aggrecan flux

set to $f = 2 \times 10^{-9} - 10^{-9}\, c^{agg}$, as this value gives the experimentally observed concentration of aggrecan at the construct surface (Klein *et al.*, 2007).

The initial conditions are zero strain, zero water pressure and 0 mg/ml aggrecan within the cartilage construct. A spatially constant source term, representing the synthesis of aggrecan by chondrocytes seeded within the collagen scaffold, is set to $s^{M}_{\mathrm{agg}} = 4.3 \times 10^{-5}$ mg/ml/s (Zhang *et al.*, 2009). This term represents the net addition of aggrecan to the cartilage by volume. At equilibrium it is exactly balanced by the amount of aggrecan leaving the construct through the permeable boundary. The simulation is run until equilibrium is reached. The parameters used in this study are shown in Table 1.

3. Results

From the initial state, aggrecan production throughout the tissue causes a steady rise in concentration. Equilibrium was reached after 48days. The steady-state distribution of aggrecan that forms can be seen in Figure 2. The concentration of aggrecan at the permeable boundary is less than one-third that at the base (19.3 mg/ml compared to 61.7 mg/ml) and rises rapidly through the first 0.5 mm of the tissue measured from the top permeable surface. Note also (shown in Figure 2 for comparison) the experimental data provided Klein *et al.* (2007) for newborn calf cartilage, i.e. a concentration of ~30 mg/ml near the cartilage surface, rising to ~60 mg/ml 1 mm below the cartilage surface. (Figure 3)

All of the plots display quantities at 6 day intervals. The osmotic pressure within the tissue is observed to increase along with the aggrecan, as expected from equation (13). The model predicts an almost linear increase in the osmotic pressure from the top permeable surface moving down through the first ~0.5 mm, with the rate of increase in osmotic pressure decreasing in the lower half of the construct.

The osmotic pressure induces a body force in the cartilage which causes an increase in collagen stress and strain, and thus causes an expansion of the tissue (refer to Figures 4, 5).

Water is drawn into the tissue construct as it expands. The movement of water and aggrecan relative to each other causes a pressure within the tissue at equilibrium. Based on the model parameters, we predict that aggrecan-induced cartilage swelling in the normal cartilage collagen network would be, at most, only a few percent (Figure 5). (Figure 6)

The ability of cartilage to resist compressive load in equilibrium is due to the swelling pressure associated with osmotic and electrostatic interactions due to aggrecan, along with non-electrostatic/osmotic contributions associated with other matrix constituents. This osmotic modulus, as described in Section 2.2.7., is plotted in Figure 7.

4. Discussion

As shown in Figure 2, the aggrecan concentration in the construct increases from zero (the initial condition in the decellularized matrix) to a profile with a high concentration in the deep middle and deep zones and a drop in concentration as we move towards the superficial zone with its permeable boundary. This equilibrium state of the model is consistent with the known depth-dependent concentration of aggrecan in immature (fetal and newborn bovine calf; Klein *et al.*, 2007) as well as adult (Maroudas,1979) articular cartilage. Klein *et al.* (2007) reported GAG concentration of ~30 mg/ml near the surface, rising to ~60 mg/ml 1 mm below the surface (newborn calf), similar to the values in Figure 2 for the parameter values used in Table 1.

Figure 3 shows the aggrecan-associated osmotic pressure within the tissue, calculated from equation (13), a major determinant of the construct mechanical and physicochemical behaviour. The collagen stress (Figure 4) is dependent on both the osmotic pressure of Figure 3 and the excess poor water pressure; however, because the rate of expansion of the collagen during the experiment is low, there is very little excess pore water pressure generated. For this reason, the collagen stress closely matches the osmotic pressure throughout the simulation, leading to the non-uniform collagen strain profile of Figure 5. It is worth noting that many poroelastic cartilage models attempt to represent the non-linear material behaviour of cartilage instead by using complex non-linear material models (e.g. Huang *et al.*, 2003; Korhonen *et al.*, 2003; Soulhat *et al.*, 1999; Wilson *et al.*, 2004; Zhang *et al.*, 2008), whereas here complex (non-linear and spatial varying) behaviour `naturally' arises as the collagen, aggrecan and interstitial fluid interact. Note that the predicted collagen strain of a few percent is consistent with experimental findings in which incubation of cartilage plugs in high salt (1 M NaCl) reduced swelling by < 2% (Eisenberg and Grodzinsky, 1985).

An excess pore water pressure develops during the temporal evolution of this quasistatic steady state (Figure 6), which becomes more negative with depth, suggesting a net inward flow of water into the tissue. However, there is no net movement of water through the tissue at equilibrium. The small negative water pressure within the tissue has its origin in the drag of the aggrecan on the water phase as the aggrecan slowly migrates from the tissue construct. The residual water pressure results from the continual production of aggrecan and its transport out of the tissue. Although not shown in Figure 6, the water pressure generated at equilibrium predicted by our model is dependent on the permeability of the water through the aggrecan. The lower the permeability of the aggrecan to water, or the greater the amount of aggrecan produced, the greater the steady-state negative pressure required to resist the drag produced by the aggrecan movement.

The osmotic modulus, as described in Section 2.2.7., provides us with a prediction of compressive stiffness due to the aggrecan. The depth-dependent plot of osmotic modulus is shown in Figure 7. From this we can see that the osmotic modulus at equilibrium increases from ~50 kPa 0.1 mm below the surface to ~200 kPa 1 mm below the surface. Klein *et al.* (2007) measured the depth-dependent `aggregate modulus' of fetal and newborn bovine cartilage in compression. Table 2 shows the measurements predicted by Klein *et al.* compared to the values predicted by our model.

The model predicts osmotic moduli that are greater than the aggregate tissue modulus measured in fetal calf cartilage, and are lower than those measured in the newborn cartilage. Comparison of model predictions to experimental data (Table 2) suggest that the osmotic modulus is the major contributor to the overall equilibrium modulus of the intact tissue. Figure 8 compares the osmotic modulus predicted by the model with the line of best fit for the aggregate modulus measured by Klein *et al.* (2007). The variation in the data measured by Klein *et al.* is much greater than the difference between the model prediction and the fit. It should also be noted that the osmotic modulus is not exactly equal to the aggregate modulus, as there are other components in the cartilage, i.e. collagen, elastin etc., which contribute to the aggregate modulus. However, aggrecan is the dominant contributor to the modulus, which allows this comparison.

The main aim of the simplified model presented here is to illustrate, through a specific problem with associated assumptions and material laws, an implementation of the general cartilage model. With this simple model we were able to demonstrate how the synthesis of aggrecan and its transport through the cartilage, and a resistance at the cartilage boundary (introduced by the Robin boundary condition), leads to a concentration gradient consistent

with experiments. However, by explicitly separating the equations describing collagen and aggrecan, the model predicted that a depth-dependent variation in collagen strain develops within the tissue from an initially isotropic matrix and cell seeding/synthesis. Of course, this is still a simple model and there are a number of additional depth-dependent variables that could be included within the model to improve the accuracy of the output or to better capture known features of cartilage. For example, the production rate of aggrecan is known to vary with depth (Buschmann *et al.*, 1996; Maroudas, 1979). The orientation, and relative proportion, of collagen is also depth-dependent (Clark, 1990) and changes during development (Hunziker *et al.*, 2007; van Turnhout *et al.*, 2010). Incorporating the variation in collagen content and orientation would require changing the isotropic material law currently employed to an anisotropic law. Variable collagen orientation would also result in depth-dependent changes to aggrecan permeability, affecting aggrecan concentration, osmotic pressure and, ultimately, the compressive modulus of the tissue model. An in-depth study of the interaction of the depth-dependent quantities would likely demonstrate how observed aggrecan profiles, for example, could be achieve in a variety of ways. Although this study would be very valuable, as it would help to elucidate what combination of factors lead to cartilage homeostasis with functional mechanical properties, and so what might be required of an engineered scaffold, it is beyond the scope of the current study.

More broadly, the proposed general continuum formulation of cartilage ECM enables the strain of the individual material components within the ECM to be followed over time, as the individual material components are synthesized, assembled and incorporated within the ECM, or lost through passive transport or degradation. Therefore, it should naturally capture the effect of time-dependent changes of ECM composition on the deformation and internal stress states of the ECM, rather than specifying a new and continually updated constitutive law in an evolving cartilage. Critically, by being more explicit about how the main components of the cartilage matrix interact, specifically taking the `solid phase' in current cartilage models and separating it into collagen and aggrecan phases, we have turned the focus on questions like: how do these elements interact and what determines their turnover? We believe these questions are central to understanding cartilage in health and in disease, as well as being central to improving strategies for cartilage tissue engineering. We would argue that there is still no unified `story' of how cartilage `works' as a prestressed biocomposite material in the cartilage literature. The proposed model gives the theoretical framework to begin to develop this story.

Acknowledgments

The authors would like to acknowledge funding received from the Australian Research Council (Grant No. ARC DP0988001), the National Health and Medical Research Council (Grant No. APP 1051538), and the National Institutes of Health (NIH; Grant No. AR60331).

References

Bathe M, Rutledge GC, Grodzinsky AJ, et al. Osmotic pressure of aqueous chondroitin sulfate solution: a molecular modeling investigation. Biophys J. 2005; 89(4):2357–2371. [PubMed: 16055525]

Biot MA. Mechanics of deformation and acoustic propagation in porous media. J Appl Phys. 1962; 33(4):1482–1498.

Buschmann MD, Grodzinsky AJ. A molecular model of proteoglycan-associated electrostatic forces in cartilage mechanics. J Biomech Eng. 1995; 117(2):179–192. [PubMed: 7666655]

Buschmann MD, Maurer AM, Berger E, et al. A method of quantitative autoradiography for the spatial localization of proteoglycan synthesis rates in cartilage. J Histochem Cytochem. 1996; 44(5):423–431. [PubMed: 8627000]

Clark JM. The organisation of collagen fibrils in the superficial zones of articular cartilage. J Anat. 1990; 171(1):117–130. [PubMed: 2081698]

Coletti JM, Akeson WH, Woo SLY. A comparison of the physical behavior of normal articular cartilage and the arthroplasty surface. J Bone Joint Surg. 1972; 54(1):147–160. [PubMed: 4262361]

Comper, WD. Cartilage: Molecular Aspects. Taylor & Francis; London: 1991. Physicochemical aspects of cartilage extracellular matrix; p. 59-96.

Comper WD, Lyons KC. Non-electrostatic factors govern the hydrodynamic properties of articular cartilage proteoglycan. Biochem J. 1993; 289:543–547. [PubMed: 8424796]

Cryer CW. A comparison of the three-dimensional consolitation theories of Biot and Terzaghi. Q J Mech Appl Math. 1963; 16(4):401–412.

DiMicco MA, Sah RL. Dependence of cartilage matrix composition on biosynthesis, diffusion, and reaction. Transport Porous Media. 2003; 50(1):57–73.

Dreier R. Hypertrophic differentiation of chondrocytes in osteoarthritis: the developmental aspect of degenerative joint disorders. Arthritis Res Ther. 2010; 12(5):216. DOI: 10.1186/ar3117. Epub 2010 Sep 16. [PubMed: 20959023]

Eisenberg SR, Grodzinsky AJ. Swelling of articular cartilage and other connective tissues: electromechanochemical forces. J Orthop Res. 1985; 3(2):148–159. [PubMed: 3998893]

Eisenberg SR, Grodzinsky AJ. The kinetics of chemically induced nonequilibrium swelling of articular cartilage and corneal stroma. J Biomech Eng. 1987; 109(1):79–89. [PubMed: 3560885]

Eyre DR, Weis MA, Wu JJ. Articular cartilage collagen: an irreplaceable framework? Eur Cell Mater. 2006; 12:57–63. [PubMed: 17083085]

Franzen A, Heinegard D. Extraction and purification of proteoglycans from mature bovine bone. Biochem J. 1984; 224:47–58. [PubMed: 6508769]

Ghanavi P, Kabiri M, Doran M. The rationale for using microscopic units of a donor matrix in cartilage defect repair. Cell Tissue Res. 2012; 347(3):643–648. [PubMed: 22327437]

Gilmore RS, Palfrey AJ. Chondrocyte distribution in the articular cartilage of human femoral condyles. J Anat. 1988; 157:23–31. [PubMed: 3198480]

Gong YY, Xue JX, Zhang WJ, et al. A sandwich model for engineering cartilage with acellular cartilage sheets and chondrocytes. Biomaterials. 2011; 32(9):2265–2273. [PubMed: 21194746]

Gordon M, Hahn R. Collagens. Cell Tissue Res. 2010; 339(1):247–257. [PubMed: 19693541]

Grogan SP, Sovani S, Pauli C, et al. Effects of perfusion and dynamic loading on human neocartilage formation in alginate hydrogels. Tissue Eng Part A. 2012; 18(17–18):1784–1792. [PubMed: 22536910]

Hascall, VC.; Luyton, FP.; Plaas, AHK., et al. Methods in Cartilage Research. Academic Press; San Diego, CA: 1990. Steady-state metabolism of proteoglycans in bovine articular cartilage; p. 108-112.

Hayes WC, Mockros LF. Viscoelastic properties of human articular cartilage. J Appl Physiol. 1971; 31(4):562–568. [PubMed: 5111002]

Heinegård D. Proteoglycans and more – from molecules to biology. Int J Exp Pathol. 2009; 90(6):575–586. [PubMed: 19958398]

Heinegard D, Paulsson M, Inerot S, et al. A novel low-molecular-weight chondroitin sulphate proteoglycan isolated from cartilage. Biochem J. 1981; 197:355–366. [PubMed: 6798963]

Horkay F, Basser PJ, Hecht AM, et al. Gel-like behavior in aggrecan assemblies. J Chem Phys. 2008; 128(13):135103. [PubMed: 18397110]

Huang CY, Soltz MA, Kopacz M, et al. Experimental verification of the roles of intrinsic matrix viscoelasticity and tension-compression nonlinearity in the biphasic response of cartilage. J Biomech Eng Trans ASME. 2003; 125(1):84–93.

Hunziker EB, Kapfinger E, Geiss J. The structural architecture of adult mammalian articular cartilage evolves by a synchronized process of tissue resorption and neoformation during postnatal development. Osteoarthr Cartilage. 2007; 15(4):403–413.

Hunziker EB, Rosenberg LC. Repair of partial-thickness defects in articular cartilage: cell recruitment from the synovial membrane. J Bone Joint Surg. 1996; 78(5):721–733. [PubMed: 8642029]

Huyghe JM, Janssen JD. Quadriphasic mechanics of swelling incompressible porous media. Int J Eng Sci. 1997; 35(8):793–802.

Kang H, Peng J, Lu S, et al. *In vivo* cartilage repair using adipose-derived stem cell-loaded decellularized cartilage ECM scaffolds. J Tissue Eng Regen Med. 2012 DOI: 10.1002/term.1538.

Kheir E, Stapleton T, Shaw D, et al. Development and characterization of an acellular porcine cartilage bone matrix for use in tissue engineering. J Biomed Mater Res A. 2011; 99A(2):283–294. [PubMed: 21858917]

Kisiday JD, Jin M, DiMicco MA, et al. Effects of dynamic compressive loading on chondrocyte biosynthesis in self-assembling peptide scaffolds. J Biomech. 2004; 37(5):595–604. [PubMed: 15046988]

Klein TJ, Chaudhry M, Bae WC, et al. Depth-dependent biomechanical and biochemical properties of fetal, newborn, and tissue-engineered articular cartilage. J Biomech. 2007; 40(1):182–190. [PubMed: 16387310]

Korhonen RK, Laasanen MS, Töyräs J, et al. Fibril reinforced poroelastic model predicts specifically mechanical behavior of normal, proteoglycan depleted and collagen degraded articular cartilage. J Biomech. 2003; 36(9):1373–1379. [PubMed: 12893046]

Lai WM, Hou JS, Mow VC. A triphasic theory for the swelling and deformation behaviors of articular cartilage. J Biomech Eng. 1991; 113(3):245–258. [PubMed: 1921350]

Lu XL, Sun DDN, Guo XE, et al. Indentation determined mechanoelectrochemical properties and fixed charge density of articular cartilage. Ann Biomed Eng. 2004; 32(3):370–379. [PubMed: 15095811]

Luscombe M, Phielps CF. The Composition and Physicochemical Properties of Bovine Nasal-Septa Protein-Polysaccharide Complex. Biochem J. 1967; 102:110–119. [PubMed: 4226525]

Maroudas, A. Adult Articular Cartilage – Physiochemical Properties of Articular Cartilage. 2nd edn.. Pitman; Tunbridge Wells, UK: 1979. p. 215-290.

Minehara H, Urabe K, Naruse K, et al. A new technique for seeding chondrocytes onto solvent-preserved human meniscus using the chemokinetic effect of recombinant human bone morphogenetic protein-2. Cell Tissue Bank. 2011; 12(3):199–207. [PubMed: 20556521]

Morales TI. Chondrocyte moves: clever strategies? Osteoarthr Cartilage. 2007; 15(8):861–871.

Mow VC, Holmes MH, Lai WM. Fluid transport and mechanical properties of articular cartilage: a review. J Biomech. 1984; 17(5):377–394. [PubMed: 6376512]

Mow VC, Kuei SC, Lai WM, et al. Biphasic creep and stress relaxation of articular cartilage in compression: theory and experiments. J Biomech Eng. 1980; 102(1):73–84. [PubMed: 7382457]

Nagase H, Kashiwagi M. Aggrecanases and cartilage matrix degradation. Arthritis Res Ther. 2003; 5(2):94–103. [PubMed: 12718749]

Ng KW, Wanivenhaus F, Chen T, et al. A novel macroporous polyvinyl alcohol scaffold promotes chondrocyte migration and interface formation in an *in vitro* cartilage defect model. Tissue Eng Part A. 2012; 18(11–12):1273–1281. [PubMed: 22435602]

Ng L, Grodzinsky AJ, Patwari P, et al. Individual cartilage aggrecan macromolecules and their constituent glycosaminoglycans visualized via atomic force microscopy. J Struct Biol. 2003; 143(3):242–257. [PubMed: 14572479]

Saha AK, Kohles SS. A cell–matrix model of anabolic and catabolic dynamics during cartilage biomolecule regulation. Int J Comput Healthcare. 2012; 1(3):214–228.

Sandy JD, O'Neill JR, Ratzlaff LC. Acquisition of hyaluronate-binding affinity *in vivo* by newly synthesized cartilage proteoglycans. Biochem J. 1989; 258(3):875–880. [PubMed: 2730571]

Schinagl RM, Gurskis D, Chen AC, et al. Depth-dependent confined compression modulus of full-thickness bovine articular cartilage. J Orthop Res. 1997; 15(4):499–506. [PubMed: 9379258]

Simkin PA. A biography of the chondrocyte. Ann Rheum Dis. 2008; 67(8):1064–1068. [PubMed: 18245112]

Soulhat J, Buschmann MD, Shirazi-Adl A. A fibril-network-reinforced biphasic model of cartilage in unconfined compression. J Biomech Eng. 1999; 121(3):340–347. [PubMed: 10396701]

van Turnhout MC, Schipper H, Engel B, et al. Postnatal development of collagen structure in ovine articular cartilage. BMC Dev Biol. 2010; 10:16. [PubMed: 20158901]

Verzijl N, DeGroot J, Thorpe SR, et al. Effect of collagen turnover on the accumulation of advanced glycation end products. J Biol Chem. 2000; 275(50):39027–39031. [PubMed: 10976109]

Wilson W, van Donkelaar CC, van Rietbergen B, et al. Stresses in the local collagen network of articular cartilage: a poroviscoelastic fibril-reinforced finite element study. J Biomech. 2004; 37(3):357–366. [PubMed: 14757455]

Zhang L, Gardiner B, Smith D, et al. Integrated model of IGF-I-mediated biosyn-thesis in a deformed articular cartilage. J Eng Mech. 2009; 135(5):439–449.

Zhang L, Gardiner BS, Smith DW, et al. The effect of cyclic deformation and solute binding on solute transport in cartilage. Arch Biochem Biophys. 2007; 457(1):47–56. [PubMed: 17107655]

Zhang L, Gardiner BS, Smith DW, et al. A fully coupled poroelastic reactive-transport model of cartilage. Mol Cell Biomech. 2008; 5(2):133–153. [PubMed: 18589501]

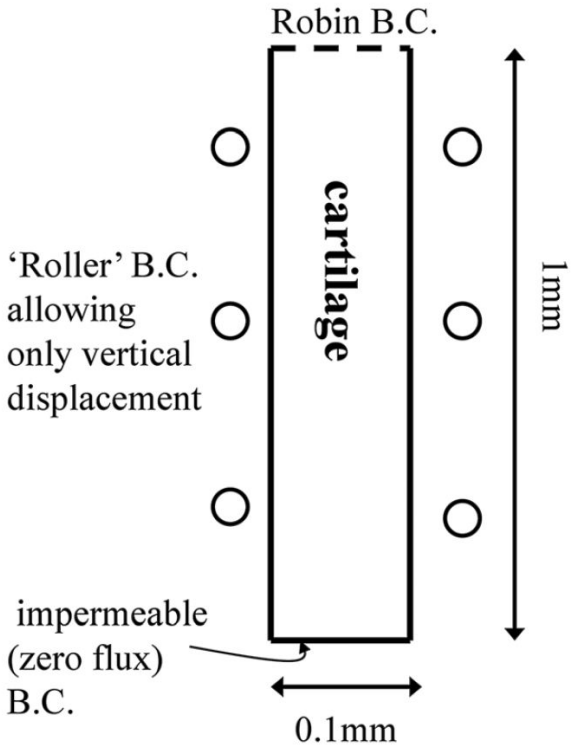

Figure 1.
Simulation geometry

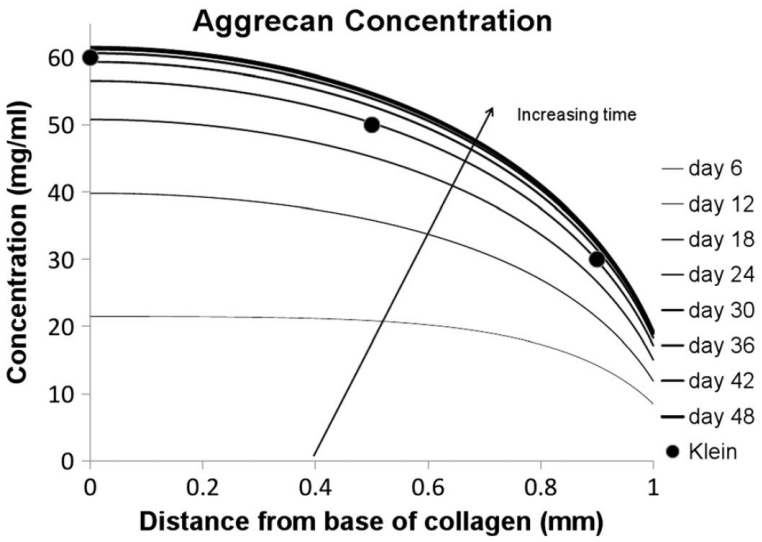

Figure 2.
Aggrecan concentration

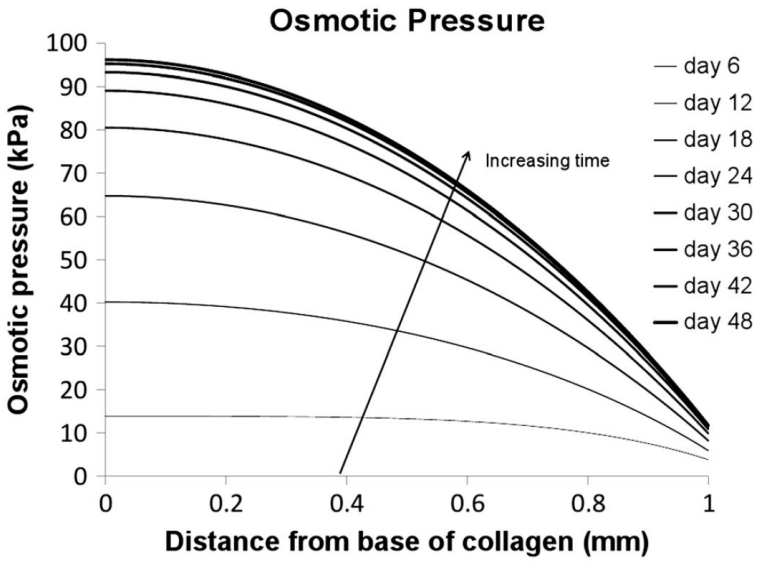

Figure 3.
Osmotic pressure

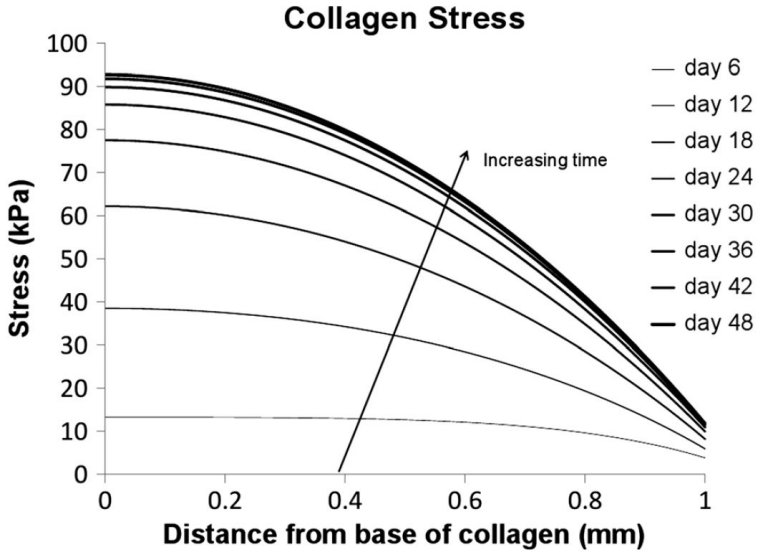

Figure 4.
Collagen stress

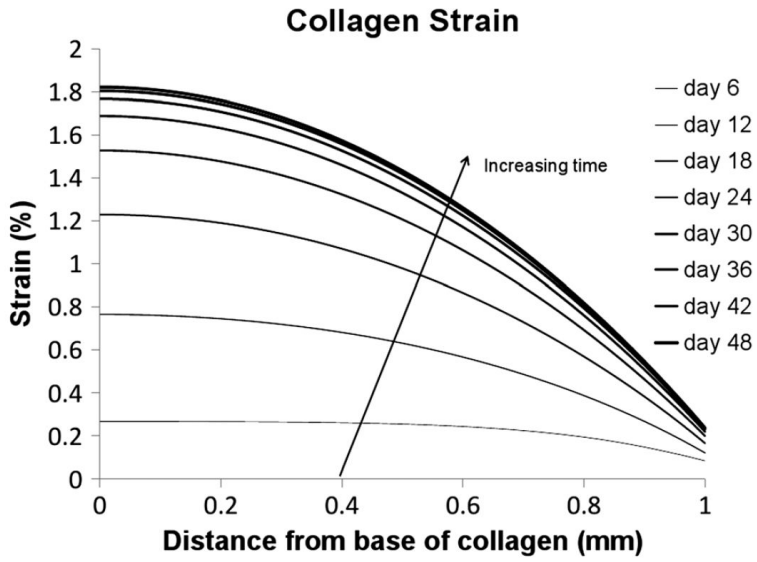

Figure 5.
Collagen strain

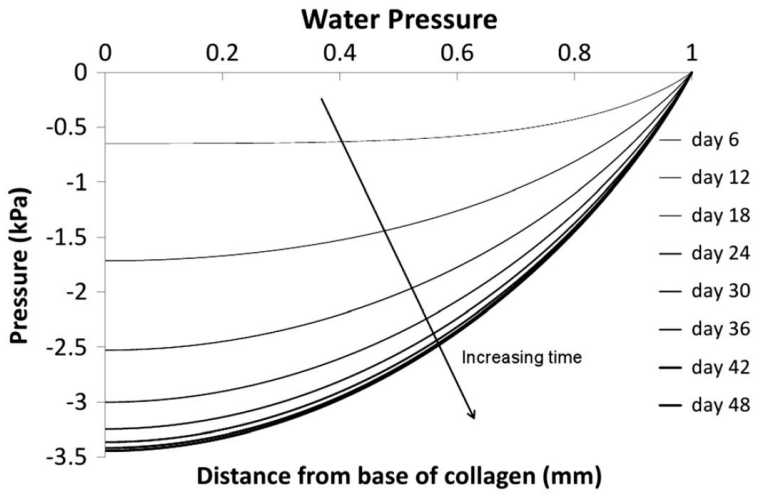

Figure 6.

Excess water pressure. This pressure arises from the drag force created from the exit of aggrecan from the tissue (refer to Discussion)

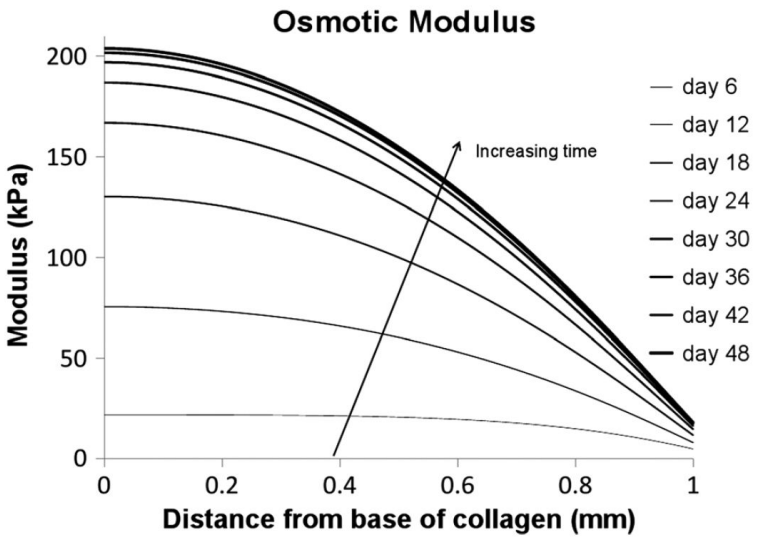

Figure 7.
Osmotic modulus

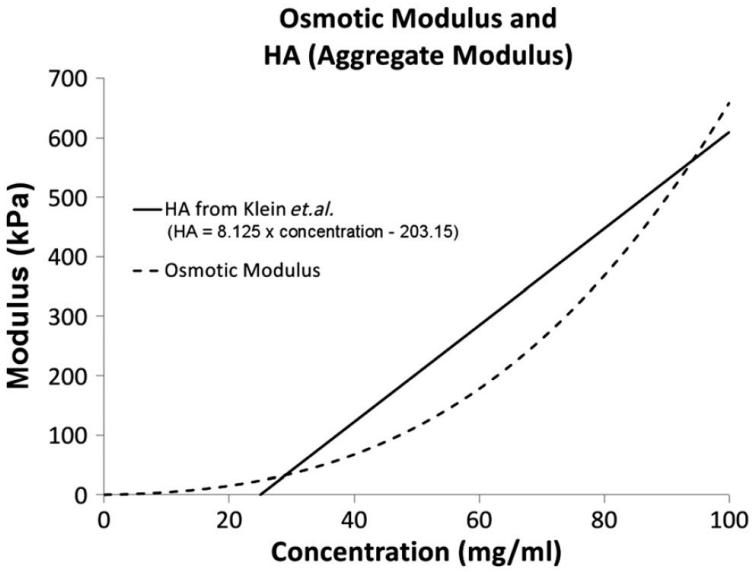

Figure 8.

Comparison between the osmotic modulus predicted in the model and the best fit to the aggregate modulus data of Klein *et al.* (2007)

Table 1

Model parameters used in this study

Parameter	Value	Reference
E_{col}	5 MPa (> 0) 0.5 MPa (< 0)	Bathe *et al.* (2005)
α_1	1.4×10^{-4}M/g	Bathe *et al.* (2005)
α_2	4.4×10^{-6}M/g^2	Bathe *et al.* (2005)
α_3	5.7×10^{-8}M^2/g^3	Bathe *et al.* (2005)
k_w	$1.02 \times 10^{-12}/c^{\text{agg}\,1.559}$ m^2/Pa/s	Comper (1993) (curve fitted)
k_{agg}	$2.7 \times 10^{-17}/c^{\text{agg}}$ m^2/Pa/s (minimum 4×10^{-18}m^2/Pa/s)	
$s^{\text{M}}_{\text{agg}}$	4.3×10^{-5}mg/ml/s	Zhang *et al.* (2009)

Note: the permeability of aggrecan (k^{agg}) is assumed to be of a similar form to the permeability of water. The values of the aggrecan permeability (and the Robin boundary condition) were not available in the literature. In this simulation these values were chosen to give the appropriate aggrecan tissue concentration, as defined by the work of Klein et *al.* (2007).

Table 2

Compressive aggregate moduli as reported by Klein *et al.* (2007) and osmotic modulus predicted by our model

Depth from cartilage surface (mm)	Klein: fetal calf aggregate (tissue) modulus (kPa)	Klein: newborn calf aggregate (tissue) modulus (kPa)	Model osmotic modulus (kPa)
0.1	28 ± 13	141 ± 10	50.4
1.0	150	600 ± 300	205.7